

**1<sup>st</sup> International Congress of Serbian Society of  
Mechanics, 10-13<sup>th</sup> April, 2007, Kopaonik**

---



# PROCEEDINGS

**Editors**

**Dragoslav Šumarac and Dragoslav Kuzmanović**

**April 10-13, 2007. Kopaonik, Serbia**

## **1<sup>st</sup> International Congress of Serbian Society of Mechanics**

### **Editors**

Prof. Dragoslav Šumarac  
Prof. Dragoslav Kuzmanović

### **Computer editing**

Nataša Trišović

### **Press**

"BeoTele Prom", Beograd

### **Circulation**

300 copies

CIP - Каталогизација у публикацији  
Народна библиотека Србије, Београд

531/534(082)

SERBIAN Society of Mechanics (Beograd).  
International Congress (1 ; 2007 ; Kopaonik)

Proceedings / 1st International Congress of Serbian Society of Mechanics,  
10-13th April, 2007, Kopaonik ; editors Dragoslav Šumarac and Dragoslav Kuzmanović. -  
Belgrade : Serbian Society of Mechanics,  
2007 (Beograd : BeoTeleProm). - XX, 1152 str. : ilustr. ; 24 cm

Tiraž 300. - Str. III: Preface / D. [Dragoslav] Šumarac & D. [Dragoslav] Kuzmanović-  
Registar. - Abstracts. - Bibliografija uz svaki rad.

ISBN 978-86-909973-0-5

а) Механика - Зборници  
COBISS.SR-ID 138952460

**Published by Serbian Society of Mechanics, Belgrade**

<http://www.ssm.org.yu/>



## FINITE ELEMENT MODEL FOR THE STATIC ANALYSIS OF LAMINATED COMPOSITE AND SANDWICH PLATES

M. Cetkovic<sup>1</sup>

<sup>1</sup> Faculty of Civil Engineering,  
The University of Belgrade, Bul. kralja Aleksandra 73, 11000 Belgrade, Serbia  
e-mail: [marina@grf.bg.ac.yu](mailto:marina@grf.bg.ac.yu)

**ABSTRACT:** Finite element model for the static analysis of laminated composite and sandwich plates, based on Generalized Laminate Plate Theory (**GLPT**) is presented in this paper. Within each layer, the theory assumes piece-wise variation of in-plane displacement components, constant transverse displacement component and parabolic distribution of shear stresses, thus accurately modeling the warping of cross section and including the effects of transverse shear deformation. Transverse shear stresses satisfy Hook's law, 3D equilibrium equations and traction free boundary conditions. Using the assumed displacement field, linear strain-displacement relations and 3D constitutive equations of lamina, equilibrium equations are derived according to the principle of virtual displacements. In the finite element formulation, in-plane displacement components are through the thickness approximated using two-node linear 1D Lagrangian finite element, while the four and nine node 2D Lagrangian elements are used for approximation of displacements in plane. Numerical results for bending stresses, transverse shearing stresses and displacements are presented, showing the parametric effect of plate aspect ratio, side-to-thickness ratio, lamination angle schemes and degree of orthotropy. The accuracy of the results is verified with the 3D elasticity theory, Higher-order Shear Deformation Theory (**HSDT**), First-order Shear Deformation Theory (**FSDT**) and Classical Laminated Plate Theory (**CLPT**) available in the literature. It has been shown that **GLPT** finite element gives excellent agreement with 3D elasticity theory and may be used in the future linear and nonlinear analysis of laminated composites.

**Key words:** composite plates, shear deformation, finite element model

### 1. Introduction

The extensive use of fibrous composite materials in different industrial fields, such as in aircraft and aerospace industry, automobile industry, sporting goods, offshore structures, and civil engineering applications, has stimulated interest in accurate prediction of their structural behavior. Despite of excellent mechanical properties like high strength-to-weight and high stiffness-to-weight ratio, the low ratio of transverse shear modulus to in-plane tensile modulus make anisotropic plates more susceptible to transverse shear deformation, than isotropic plates. Furthermore, transverse discontinuous mechanical properties cause displacement field  $(u_1, u_2, u_3)$  in the thickness direction which can exhibit a rapid change of their slopes in correspondence to each layer interface. This is known as *zigzag effects*. Also transverse stresses  $(\tau_{xz}, \tau_{yz}, \sigma_{zz})$ , for equilibrium reasons, must fulfill interlaminar continuity at each layer interface.

Figure 1 shows, from the qualitative point of view, displacement and transverse stress distributions in a multilayer structure. Both displacements and transverse stresses are  $C^0$  continuous functions in thickness  $z$  direction, while displacements and transverse stresses field have, in the general, discontinuous first derivatives with correspondence to each interface where mechanical properties change. The fulfillment of  $C_z^0$ -requirements is a crucial point of two dimensional modeling of multilayered structures.

Many refined theories originally developed for homogeneous isotropic thin, moderately thick and very thick plates are extended to laminated anisotropic plates and also new refined shear deformation theories are developed for accurate analysis of anisotropic laminated composites. All these theories are divided into two categories: 1) Equivalent single layer theories (ESL) such as: Classical Laminate Plate Theory (CLPT), First-order Shear Deformation Theory (FSDT) and Higher order Shear Deformation Theories (HSDT) and 2) Discrete layer theories or layerwise theories (LWT).

The theories based on the equivalent single layer approach, are developed by expanding the displacement

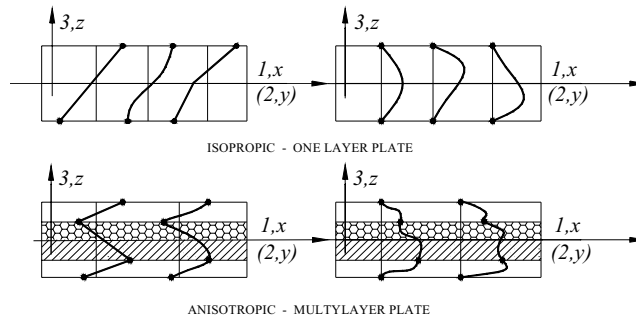


Fig. 1. The  $C_z^0$  requirements. Comparison of displacement and transverse stress field between one-layer and four layer structures.

field in a power series expansion through the thickness coordinate. The Classical Laminate Plate Theory (CLPT), based on the Kirchhoff hypothesis neglects the transverse shear deformation, and is therefore limited to only thin plates. The theory is based on a linear displacement across the entire laminate. In First-order Shear Deformation Theory (FSDT) shear correction factor is required to account for strain energy of shear deformation. These factors depend upon the ply properties, ply lay-up, fiber orientation, boundary conditions, and the particular application. It is also known that these factors for multilayered composite plates are different from those of homogeneous plates. The limitations of classical and first order laminated plate theories forced the development of single layer models based on Higher order Shear Deformation Theories (HSDT). These models involve higher order expansions of displacement field in powers of the thickness coordinate, giving the quadratic variation of out-of plane strains and therefore not requiring the use of artificial shear correction factors. In all equivalent single layer (ESL) theories, transverse shear stresses obtained by using the constitutive relations are discontinuous at the interfaces between the layers which are contradictory against the equilibrium conditions. Thus many authors suggested the use of three-dimensional equilibrium equations to obtain the transverse stresses through the thickness of the laminate.

To overcome the drawbacks of equivalent single layer theories, layerwise theories have been proposed. These theories are divided into two categories depending on the number on unknowns in the kinematical model that is 1) Layer dependent theories and 2) Layer independent theories. Layer independent theories are discrete layer theories in which the number of unknowns in the model does not depend on the number of layers in the laminate. In all these theories a piecewise (linear, cubic, etc.) displacement function is superimposed over the linear displacement field. In layer dependent theories number of unknowns in the model is dependent on the number of layers. They could account for any degree of approximation of in-plane and transverse displacement distribution through a proper selection of variables and functions.

In this paper Layer dependent theory, called Generalized Layerwise Plate Theory of Reddy is presented. The theory assumes transverse variation of the in-plane displacement components in terms of one-dimensional Lagrangian finite elements. The resulting strain field is kinematically correct in that the in-plane strains are continuous through the thickness allowing for the possibility of continuous transverse stresses. Transverse shear stresses satisfy Hook's law, 3D equilibrium equations and traction free boundary conditions and have quadratic variation within each layer of the laminate. Following the displacement based finite element formulation, the main variables are displacements  $(u, v, w)$  in the middle surface nodes and  $(U^I, V^I)$  displacements of the I-th plane nodes across the plate thickness  $(I=1, N)$ . The aim of this paper is to evaluate the accuracy of the present formulation for bending stresses, transverse shearing stresses and displacements by comparing them with 3D elasticity theory, HSDT, FSDT and CLPT results available in the literature.

## 2. Theoretical formulation

### 2.1 Displacement field

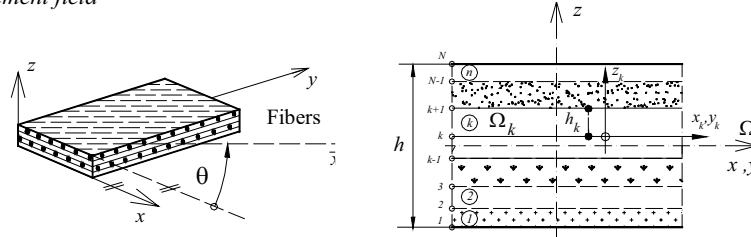


Fig. 2. Multilayer laminated plate

Consider a laminated plate (Fig. 2) composed of  $n$  orthotropic lamina. The integer  $k$  denotes the layer number that starts from the plate bottom. Plate middle surface coordinates are  $(x, y, z)$ , while layer coordinates are  $(x_k, y_k, z_k)$ . Plate and layer thickness are denoted as  $h$  and  $h_k$ , respectively. We assume that 1) the layers are perfectly bonded together, 2) the material of each layer is linearly elastic and has three planes of materials symmetry (i.e., orthotropic), 3) strains are small, 4) each layer is of uniform thickness, 5) the inextensibility of normal is imposed.

The displacements components  $(u_1, u_2, u_3)$  at a point  $(x, y, z)$  can be written as:

$$\begin{aligned} u_1(x, y, z) &= u(x, y) + \sum_{I=1}^N U^I(x, y) \cdot \Phi^I(z) \\ u_2(x, y, z) &= v(x, y) + \sum_{I=1}^N V^I(x, y) \cdot \Phi^I(z), \\ u_3(x, y, z) &= w(x, y) \end{aligned} \quad (1)$$

where  $(u, v, w)$  are the displacements of a point  $(x, y, 0)$  on the reference plane of the laminate,  $U^I$  and  $V^I$  are undetermined coefficients, and  $\Phi^I(z)$  are layerwise continuous functions of the thickness coordinate. In the view of finite element approximation, the functions  $\Phi^I(z)$  are the one-dimensional (linear, quadratic or cubic) Lagrange interpolation functions of the thickness coordinates and  $(U^I, V^I)$  are the values of  $(u_1, u_2)$  at the I-th plane. If we assume linear Lagrange interpolation of in-plane displacement components through the thickness, it could be recognized that each layer is in fact a 1D finite element and that the in-plane displacements are piece-wise continuous through the laminate thickness.

## 2.2 Strain displacement relations

The strains associated with the displacement field are as follows:

$$\{\boldsymbol{\varepsilon}^0\} = \left\{ \frac{\partial u}{\partial x} \quad \frac{\partial v}{\partial y} \quad \frac{\partial u}{\partial y} + \frac{\partial v}{\partial x} \quad \frac{\partial w}{\partial x} \quad \frac{\partial w}{\partial y} \right\}^T \quad \{\boldsymbol{\varepsilon}^I\} = \left\{ \frac{\partial U^I}{\partial x} \quad \frac{\partial V^I}{\partial y} \quad \frac{\partial U^I}{\partial y} + \frac{\partial V^I}{\partial x} \quad U^I \quad V^I \right\}^T \quad (2)$$

## 2.3 Constitutive equations

The stress-strain relations in the laminate coordinates can be written as:

$$\begin{Bmatrix} \sigma_{xx} \\ \sigma_{yy} \\ \tau_{xy} \\ \tau_{xz} \\ \tau_{yz} \end{Bmatrix}^{(k)} = \begin{bmatrix} Q_{11} & Q_{12} & Q_{13} & 0 & 0 \\ Q_{12} & Q_{22} & Q_{23} & 0 & 0 \\ Q_{13} & Q_{23} & Q_{33} & 0 & 0 \\ 0 & 0 & 0 & Q_{44} & Q_{45} \\ 0 & 0 & 0 & Q_{45} & Q_{55} \end{bmatrix}^{(k)} \times \begin{Bmatrix} \varepsilon_{xx} \\ \varepsilon_{yy} \\ \gamma_{xy} \\ \gamma_{xz} \\ \gamma_{yz} \end{Bmatrix}^{(k)} \quad (3)$$

where  $\boldsymbol{\sigma}^{(k)} = \{\sigma_{xx} \quad \sigma_{yy} \quad \tau_{xy} \quad \tau_{xz} \quad \tau_{yz}\}^{(k)T}$  and  $\boldsymbol{\varepsilon}^{(k)} = \{\varepsilon_{xx} \quad \varepsilon_{yy} \quad \gamma_{xy} \quad \gamma_{xz} \quad \gamma_{yz}\}^{(k)T}$  are stress and strain components, respectively, of k-th lamina in global coordinates.

## 2.4 Virtual work statement

The virtual work statement can be written using Hamilton's principle:

$$0 = \int_{\Omega} \left( \{\delta \boldsymbol{\varepsilon}^0\}^T \{\mathbf{N}^0\} + \{\delta \boldsymbol{\varepsilon}^I\}^T \{\mathbf{N}^I\} - q \delta w \right) dA \quad (4)$$

where stress resultants are:

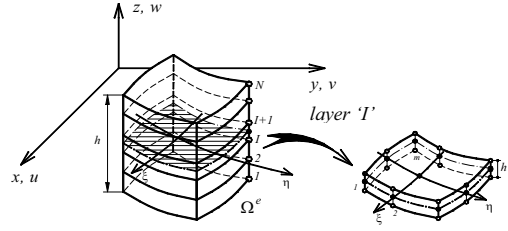
$$\{\mathbf{N}^0\} = [\mathbf{A}] \{\boldsymbol{\varepsilon}^0\} + \sum_{I=1}^N [\mathbf{B}^I] \{\boldsymbol{\varepsilon}^I\} \quad \{\mathbf{N}^I\} = [\mathbf{B}^I] \{\boldsymbol{\varepsilon}^0\} + \sum_{J=1}^N [\mathbf{D}^{IJ}] \{\boldsymbol{\varepsilon}^J\} \quad (5)$$

Constitutive matrices for the laminate are:

$$\begin{aligned} [\mathbf{A}] &= [A_{pq}] = \sum_{k=1}^n \int_{z_k}^{z_{k+1}} [Q_{pq}^{(k)}] dz, \quad p, q = 1, 2, 3, 4, 5; \\ [\mathbf{B}] &= [\overline{B}_{pq}^I] = \sum_{k=1}^n \int_{z_k}^{z_{k+1}} [Q_{pq}^{(k)}] \frac{d\Phi^I}{dz} dz, \quad p, q = 4, 5 \\ [\mathbf{D}] &= [D_{pq}^{IJ}] = \sum_{k=1}^n \int_{z_k}^{z_{k+1}} [Q_{pq}^{(k)}] \Phi^J \Phi^I dz, \quad p, q = 1, 2, 3 \\ [\mathbf{D}] &= [\overline{D}_{pq}^{IJ}] = \sum_{k=1}^n \int_{z_k}^{z_{k+1}} [Q_{pq}^{(k)}] \frac{d\Phi^J}{dz} \frac{d\Phi^I}{dz} dz, \quad p, q = 4, 5 \end{aligned} \quad (6)$$

## 3. Finite Element Model

The **GLPT** finite element consists of middle surface plane and I=1,N planes through the thickness of the plate (Fig. 3). The element requires only the  $C^0$  continuity of major unknowns, thus in each node only a displacement components are adopted, that is  $(u, v, w)$  in the middle surface element nodes and  $(U^I, V^I)$  in the I-th plane element nodes.



### 3.1 Displacement field

The generalized displacement over element  $\Omega^e$  can be expressed as:

$$\begin{Bmatrix} u \\ v \\ w \end{Bmatrix}^e = \begin{Bmatrix} \sum_{j=1}^m u_j \Psi_j \\ \sum_{j=1}^m v_j \Psi_j \\ \sum_{j=1}^m w_j \Psi_j \end{Bmatrix}^e = \sum_{j=1}^m [\Psi_j]^e \{\mathbf{d}_j\}^e, \quad \begin{Bmatrix} U^I \\ V^I \end{Bmatrix}^e = \begin{Bmatrix} \sum_{j=1}^m U_j^I \Psi_j \\ \sum_{j=1}^m V_j^I \Psi_j \end{Bmatrix}^e = \sum_{j=1}^m [\bar{\Psi}_j]^e \{\mathbf{d}'_j\}^e \quad (7)$$

where  $\{\mathbf{d}_j\}^e = \{u_j^e \ v_j^e \ w_j^e\}^T$ ,  $\{\mathbf{d}'_j\}^e = \{U_j^I \ V_j^I\}^T$  are displacement vectors in the middle plane and I-th plane, respectively and  $\Psi_j^e$  are interpolation functions, for the j-th node of the element  $\Omega^e$ .

$$[\Psi_j]^e = \begin{bmatrix} \Psi_j^e(x_j^e, y_j^e) & 0 & 0 \\ 0 & \Psi_j^e(x_j^e, y_j^e) & 0 \\ 0 & 0 & \Psi_j^e(x_j^e, y_j^e) \end{bmatrix}, \quad [\bar{\Psi}_j]^e = \begin{bmatrix} \Psi_j^e(x_j^e, y_j^e) & 0 \\ 0 & \Psi_j^e(x_j^e, y_j^e) \end{bmatrix} \quad (8)$$

### 3.2 Strain field

For the assumed linear strain-displacement relations, we have:

$$\{\boldsymbol{\varepsilon}\} = \begin{Bmatrix} \boldsymbol{\varepsilon}_b \\ \boldsymbol{\varepsilon}_s \end{Bmatrix} = \sum_{j=1}^m \begin{bmatrix} [\mathbf{H}_{bj}] \\ [\mathbf{H}_{sj}] \end{bmatrix} \{\mathbf{d}_j\}^e = \sum_{j=1}^m [\mathbf{H}_j] \{\mathbf{d}_j\}^e, \quad \{\boldsymbol{\varepsilon}'\} = \begin{Bmatrix} \boldsymbol{\varepsilon}'_b \\ \boldsymbol{\varepsilon}'_s \end{Bmatrix} = \sum_{j=1}^m \begin{bmatrix} [\bar{\mathbf{H}}_{bj}] \\ [\bar{\mathbf{H}}_{sj}] \end{bmatrix} \{\mathbf{d}'_j\}^e \quad (9)$$

where

$$[\mathbf{H}_{bj}] = \begin{bmatrix} \frac{\partial \Psi_j^e}{\partial x} & 0 & 0 \\ 0 & \frac{\partial \Psi_j^e}{\partial y} & 0 \\ \frac{\partial \Psi_j^e}{\partial y} & \frac{\partial \Psi_j^e}{\partial x} & 0 \end{bmatrix}, \quad [\bar{\mathbf{H}}_{bj}] = \begin{bmatrix} \frac{\partial \Psi_j^e}{\partial x} & 0 \\ 0 & \frac{\partial \Psi_j^e}{\partial y} \end{bmatrix}, \quad [\mathbf{H}_{sj}] = \begin{bmatrix} 0 & 0 & \frac{\partial \Psi_j^e}{\partial x} \\ 0 & 0 & \frac{\partial \Psi_j^e}{\partial y} \end{bmatrix}, \quad [\bar{\mathbf{H}}_{sj}] = \begin{bmatrix} \Psi_j^e & 0 \\ 0 & \Psi_j^e \end{bmatrix} \quad (10)$$

### 3.3 Equilibrium equations

From the equation (4) we can obtain the finite element model:

$$[\mathbf{K}]^e \{\boldsymbol{\Delta}\}^e = \{\mathbf{f}\}^e \quad (11)$$

Stiffness matrix for the element  $\Omega^e$  is:

$$[\mathbf{K}]^e = \int_{\Omega^e} \left[ \begin{array}{c} [\mathbf{H}]^T [\mathbf{A}] [\mathbf{H}] \quad \sum_{I=1}^N [\mathbf{H}]^T [\mathbf{B}^I] [\overline{\mathbf{H}}] \\ \sum_{I=1}^N [\overline{\mathbf{H}}]^T [\mathbf{B}^I] [\mathbf{H}] \quad \sum_{I=1}^N \sum_{J=1}^N [\overline{\mathbf{H}}]^T [\mathbf{D}^{IJ}] [\overline{\mathbf{H}}] \end{array} \right] d\Omega^e \quad (12)$$

Force and displacement vectors for the element  $\Omega^e$  are:

$$\{\mathbf{f}\}^e = \int_{\Omega^e} [\mathbf{\Psi}]^T \begin{Bmatrix} 0 \\ 0 \\ q \end{Bmatrix} d\Omega^e, \quad \{\Delta\}^e = \left\{ \begin{array}{c} \{\mathbf{d}\} \\ \left\{ \sum_{I=1}^N \mathbf{d}^I \right\} \end{array} \right\}^e \quad (13)$$

### 3.4 Stress field

The piece-wise linear interpolation of displacement field through the thickness provide accurate prediction of in-plane stresses ( $\sigma_{xx}, \sigma_{yy}, \tau_{xy}$ ). They can be computed from the constitutive relations:

$$\begin{aligned} \{\sigma_b\}_D^{(k)e} &= [\mathbf{Q}_b]^{(k)} \sum_{j=1}^m [\mathbf{H}_{bj}] \{\mathbf{d}_j\}^e + [\mathbf{Q}_b]^{(k)} \sum_{j=1}^m [\overline{\mathbf{H}}_{bj}] \{\mathbf{d}_j^I\}^e \\ \{\sigma_b\}_G^{(k)e} &= [\mathbf{Q}_b]^{(k)} \sum_{j=1}^m [\mathbf{H}_{bj}] \{\mathbf{d}_j\}^e + [\mathbf{Q}_b]^{(k)} \sum_{j=1}^m [\overline{\mathbf{H}}_{bj}] \{\mathbf{d}_j^{I+1}\}^e \end{aligned} \quad (14)$$

Interlaminar stresses ( $\tau_{xz}, \tau_{yz}$ ) are assumed to have quadratic distribution within each layer. They are calculated by satisfying Hook's law, 3D equilibrium equations and traction free boundary conditions.

## 4. Numerical results and discussion

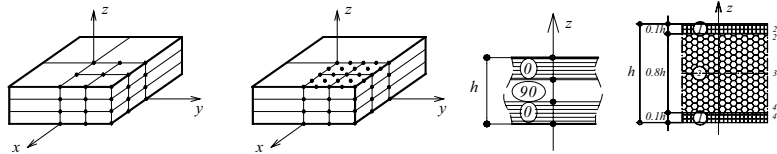


Fig. 4. Three layer orthotropic and sandwich laminated plate finite element

Numerical results are presented for four and three layer orthotropic cross ply 0/90/90/0, 0/90/0 and angle ply 45/-45/45/-45, -45/45/-45 laminated plates and three layer sandwich plate subjected to sinusoidal and uniform transverse load (Fig. 4). The plate is made of one of the following materials:

$$\text{Mat I } E_1/E_2 = 25, G_{12}/E_2 = 0.5, G_{13}/E_2 = 0.5, G_{23}/E_2 = 0.2, \nu_{12} = \nu_{13} = \nu_{23} = 0.25,$$

$$\text{Mat II } E_1/E_2 = \text{open}, G_{12}/E_2 = G_{13}/E_2 = 0.6, G_{23}/E_2 = 0.5, \nu_{12} = \nu_{13} = \nu_{23} = 0.25,$$

$$\text{Mat III } E_2/E_1 = 0.5252, G_{12}/E_1 = 0.2928, G_{23}/E_1 = 0.2972, G_{13}/E_1 = 0.1781, \nu_{12} = 0.44, \nu_{23} = 0.23$$

The laminated plates have individual layers of equal thickness, while sandwich plate has core of thickness  $h_c = 0.8h$  and flange of thickness  $h_f = 0.1h$  and  $a/h = 10$ . The transverse deflections are given in non-dimensional form, when using material I II, or II respectively.

$$\overline{w}^{(I,II)} = \frac{100E_2h^3}{qa^4} w \quad w^{(III)} = wE_1^{(2)}/hp(1 - \nu_{12}\nu_{23}) \quad (15)$$

For the interpolation of displacements in plane, linear and quadratic 2D Lagrangian interpolation functions are used, while transverse variation of in-plane displacement components



are given in terms of 1D Lagrangian finite elements. The stresses were computed at the Gauss points, closest to position where they have maximum values. The aim of the analysis is to assess the quality of the finite element model and its abilities to model laminated composite plates.

4.1 Simply supported square plate (0/90/90/0) under sinusoidal load  $q(x, y) = q \sin(\frac{\pi x}{a}) \sin(\frac{\pi y}{b})$

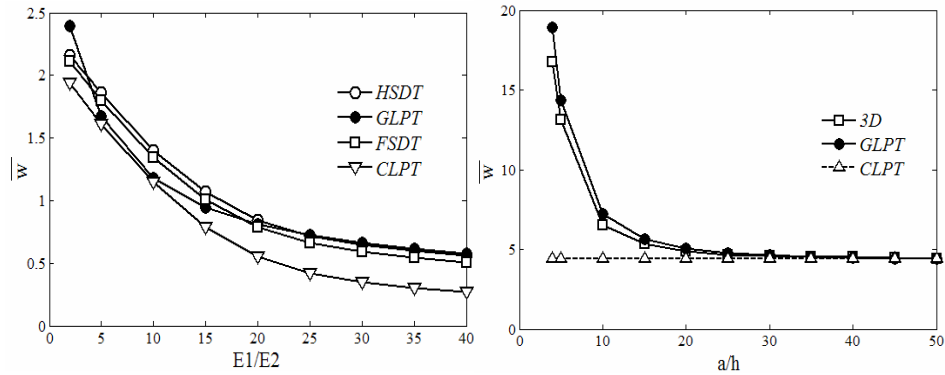


Fig. 5. Material I: a) The effect of material anisotropy ( $a/h=10$ ) and b) The side to thickness ratio on non-dimensional center deflection of cross-ply (0/90/90/0) square plate under sinusoidal load

Figure 5 shows non-dimensional center deflection  $\bar{w}$  as a function of material anisotropy of the plate and side to thickness ratio. By increasing the degree of orthotropy, deflection becomes smaller, while the effects of shear deformation become greater, giving the advantage to shear deformation theories, rather than classical plate theory (Fig. 5a). It can be seen from Fig. 5b that center deflection decreases as we approach to thin plate limit. This is because thin plate assumption increases the stiffness of the plate, thus yielding to lower deflections. In both cases **GLPT** model is in close agreement with **3D** or **HSDT** solutions.

4.2 Simply supported square plate under uniform (UDL) and sinusoidal (SSL) distributed load

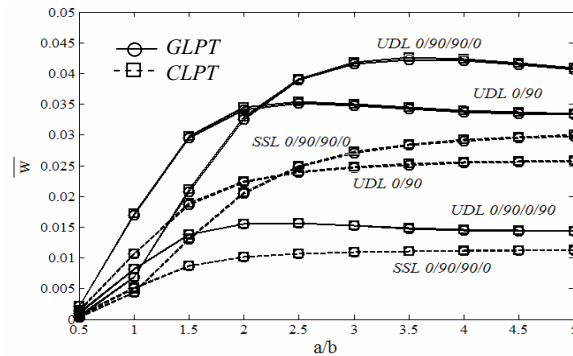


Fig. 6. Material I: a) The effect of aspect ratio on non-dimensional center deflection of simply supported square plate ( $a/h=100$ )

The effects of bending-stretching coupling on transverse deflection are shown on Figure 6. The **GLPT** results closely agree with **CLPT** results for thin plates ( $a/h=100$ ). The Figure 6 also shows that the magnitude of deflections of symmetric laminates (0/90/90/0) are about two to three times

that of anti-symmetric (0/90/0/90) laminates for  $a/b > 1$ . For uniformly distributed load there exists a ratio, around  $a/b=2.25$  for (0/90/0/90) and  $a/b=3.5$  for (0/90/90/0), for which the deflection is maximum of all ratios.

4.3 Simply supported square plate (-45/45/-45) and (45/-45/45/-45) under uniformly distributed transverse load

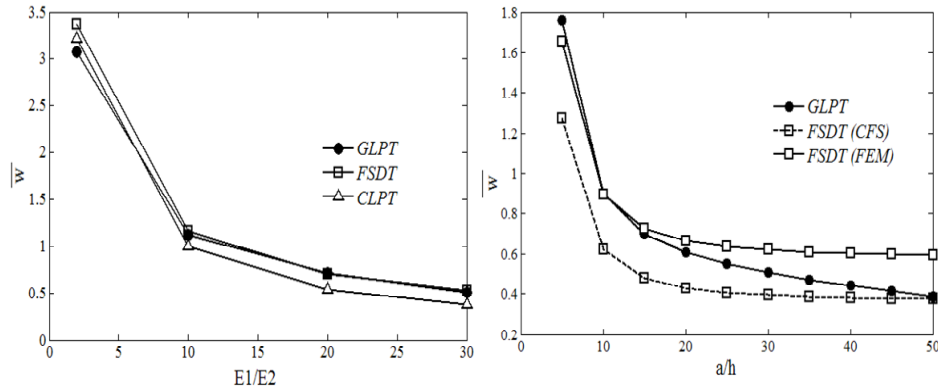


Fig. 7. a) Mat II: The effect of anisotropy of 45/-45/45/-45 and b) Mat I: The effect of side to thickness ratio of -45/45/-45 of simply supported square plate on the non-dimensional center deflection

Figure 7 contains plots of a) four layer 45/-45/45/-45 anti-symmetric laminates for different values of  $E_1/E_2$  ratio and b) three layer -45/45/-45 symmetric laminates versus side to thickness ratio. It can be seen from the Figure 7a that the increase in anisotropy ratio decreases the deflections of the plate. Also differences between closed form solution of **FSDT** and finite element solution of **GLPT** on Figure 7b can be attributed to the different representation of the shear deformation (**Closed Form Solution**, **Finite Element Model of FSDT**).

4.4 Simply supported square sandwich plate under uniformly distributed transverse load

Table 1 displays the effects of modular ratio between outer and middle plies  $\beta = E_1^{(1)}/E_1^{(2)}$  on non-dimensional center deflections, in-plane stresses and shear stresses of square sandwich plate (Mat III). We can see that as the module ratio between stiff faces and weak core increases,

Table 1. Material III: Transverse deflection and stresses of sandwich plate for different  $E_1^{(1)}/E_1^{(2)}$

| $\beta$ |               | CLPT   | 3D      | HSDT    | FEM_9   | $\beta$ | CLPT    | 3D      | HSDT    | FEM_9   |         |
|---------|---------------|--------|---------|---------|---------|---------|---------|---------|---------|---------|---------|
| 5       | $w_0$         | 216.94 | 258.97  | 256.81  | 258.68  | 15      | 81.768  | 121.72  | 114.42  | 121.70  |         |
|         | $\sigma_x/p$  | 1      | -61.141 | -60.353 | -60.330 |         | -60.275 | -69.135 | -66.787 | -66.834 | -66.713 |
|         |               | 2°     | -48.913 | -46.623 | -46.981 |         | -46.490 | -55.308 | -48.299 | -50.269 | -48.238 |
|         |               | 2°     | -9.7826 | -9.3402 | -9.3962 |         | -9.298  | -3.6872 | -3.2379 | -3.3513 | -3.216  |
|         |               | 4°     | 9.7826  | 9.2845  | 9.3962  |         | 9.298   | 3.6872  | 3.2009  | 3.3513  | 3.216   |
|         |               | 4°     | 48.913  | 46.426  | 46.981  |         | 46.490  | 55.308  | 48.028  | 50.269  | 48.238  |
|         |               | 5      | 61.141  | 60.155  | 60.330  |         | 60.275  | 69.135  | 66.513  | 66.834  | 66.713  |
|         | $\tau_{xz}/q$ | 3      | 4.5899  | 4.3641  | 4.7130  |         | 4.3817  | 4.2825  | 3.9638  | 3.9084  | 4.0090  |

classical plate theory (**CLPT**) becomes inadequate and refined mathematical models may be used. Again the **GLPT (FEM\_9)** model has excellent agreement with **3D** elasticity model.

4.5 Simply supported square plate (0/90/0) under uniformly distributed transverse load

The accuracy of results for stresses and displacements of simply supported square 0/90/0 laminated plate (Mat I) is verified by comparison of finite element results with closed form solution of the **GLPT**<sup>[4]</sup>.

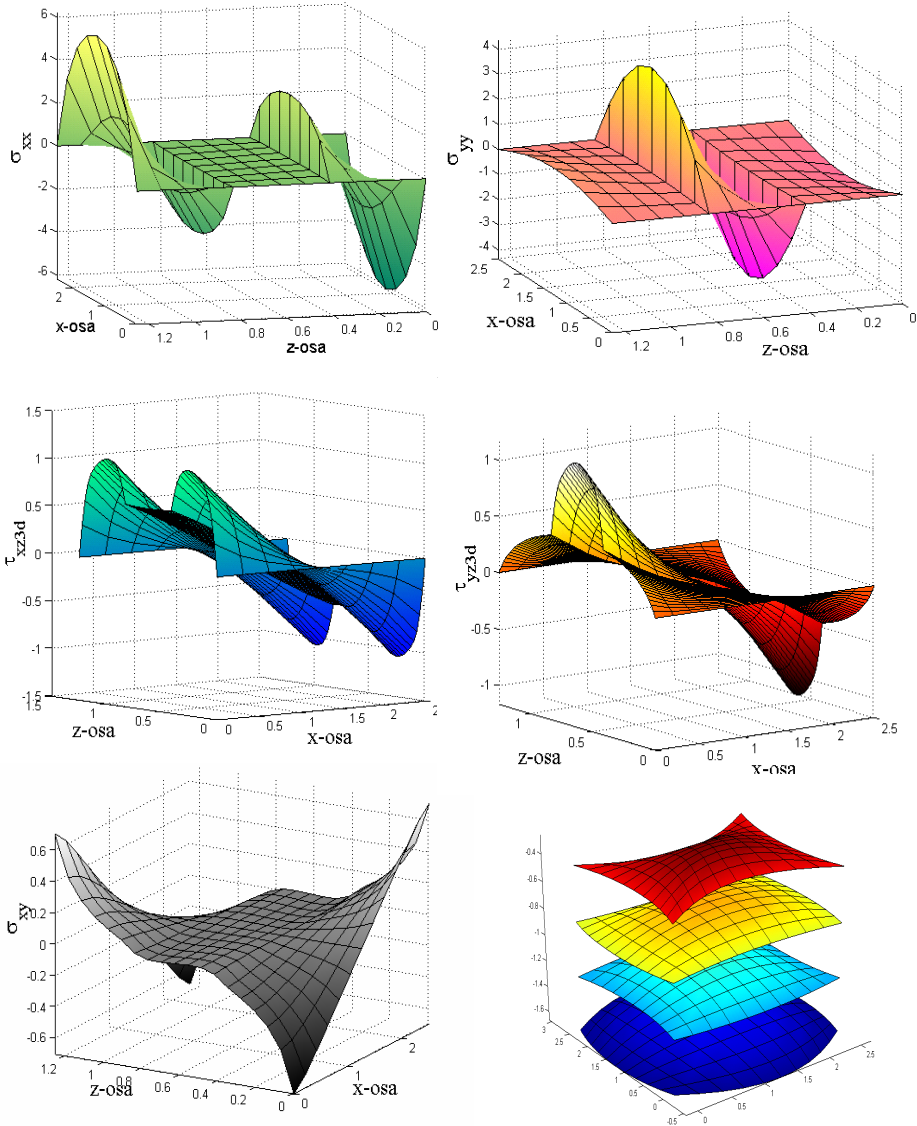


Fig. 8. Material I: Stress and deformation surfaces of 0/90/0 square laminated plate ( $a/h=2$ )

|     |     | $\tau_{yz}^{3D}$ |                        | $\tau_{xz}^{3D}$ |                        |
|-----|-----|------------------|------------------------|------------------|------------------------|
| $n$ | $N$ | MKE 9<br>4 x 4   | Analytical<br>solution | MKE 9<br>4 x 4   | Analytical<br>solution |
| 1   | 1   | 0                | 0                      | 0                | 0                      |
|     | 2   | 0.184954         | 0.187025               | 0.763926         | 0.748799               |
|     | 3   | 0.333565         | 0.326583               | 1.12738          | 1.09753                |
|     | 4   | 0.445833         | 0.418675               | 1.09037          | 1.04618                |
|     | 5   | 0.521759         | 0.463301               | 0.652897         | 0.59477                |
| 2   | 1   | 0.521759         | 0.463301               | 0.652897         | 0.59477                |
|     | 2   | 1.02153          | 0.986492               | 0.590201         | 0.58255                |
|     | 3   | 1.18811          | 1.16089                | 0.569302         | 0.578477               |
|     | 4   | 1.02153          | 0.986492               | 0.590201         | 0.58255                |
|     | 5   | 0.521759         | 0.463301               | 0.652897         | 0.59477                |
| 3   | 1   | 0.521759         | 0.463301               | 0.652897         | 0.59477                |
|     | 2   | 0.445833         | 0.418675               | 1.09037          | 1.04618                |
|     | 3   | 0.333565         | 0.326583               | 1.12738          | 1.09753                |
|     | 4   | 0.184954         | 0.187025               | 0.763926         | 0.748799               |
|     | 5   | 0                | 0                      | 0                | 0                      |
| $N$ |     | MKE 9<br>4 x 4   | Analytical<br>solution | MKE 9<br>4 x 4   | Analytical<br>solution |
|     |     | $u$              |                        | $v$              |                        |
|     | 1   | 0.1655           | 0.1655                 | 0.5697           | 0.5697                 |
|     | 2   | -0.1210          | -0.1210                | 0.1361           | 0.1361                 |
|     | 3   | 0.1210           | 0.1210                 | -0.1361          | -0.1361                |
|     | 4   | -0.1655          | -0.1655                | -0.56971         | -0.5697                |

| $N$           | MKE_9<br>4 x 4 | Analytical<br>solution |
|---------------|----------------|------------------------|
| $\sigma_{xx}$ |                |                        |
| $1^G$         | -4.9427        | -4.9054                |
| $2^D$         | 3.4210         | 3.3964                 |
| $2^G$         | 0.09894        | 0.09825                |
| $3^D$         | -0.09894       | -0.09825               |
| $3^G$         | -3.4210        | -3.3964                |
| $4^D$         | 4.9427         | 4.9054                 |
| $\sigma_{yy}$ |                |                        |
| $1^G$         | -0.6511        | -0.6475                |
| $2^D$         | -0.1233        | -0.1223                |
| $2^G$         | -3.9137        | -3.8829                |
| $3^D$         | 3.9137         | 3.8829                 |
| $3^G$         | 0.1233         | 0.1223                 |
| $4^D$         | 0.6511         | 0.6475                 |
| $\tau_{xy}$   |                |                        |
| $1^G$         | 0.5405         | 0.5280                 |
| $2^D$         | -0.003149      | -0.002052              |
| $2^G$         | -0.003149      | -0.002052              |
| $3^D$         | 0.003149       | 0.002052               |
| $3^G$         | 0.003149       | 0.0020516              |
| $4^D$         | -0.5405        | -0.5280                |

Table 2. Material I: Stress and deformation surfaces of 0/90/0 square laminated plate ( $a/h=2$ )

Table 2 shows that the finite element stress and displacement field convergence to the analytical solutions of **GLPT**<sup>[4]</sup>.

**5. Conclusion**

In this paper a displacement finite-element formulation of generalized laminated theory of Reddy is presented. It has been shown that proposed element gives excellent results for both thick and thin arbitrary laminated anisotropic plates. The result for interlaminar stress and displacement filed are closest to 3D elasticity solutions, with less computational costs, and can be used in the future failure analysis of composite laminates.

**References**

[1] Reddy, J.N., A plate bending element based on a generalized laminated plate theory, *International Journal For Numerical Methods In Engineering*, Vol. 28, 1989, pp. 2275-2292.  
 [2] Chaudhuri, R.A., *An Approximate Semi-Analytical Method For Prediction Of Interlaminar Shear Stress In Arbitrarily Laminated Thick Plate*, Composite Structures, Vol. 25, 1987., pp. 627-636  
 [3] Vuksanovic, Dj., *Linear analysis of laminated composite plates using single layer higher-order discrete models*, Composite Structures, Vol. 48, 2000., pp. 295-211.  
 [4] Cetkovic, M., *A Closed Form Solution Using a Generalized Laminte Plate Theory*, Zbornik Radova Građevinskog Fakulteta u Subotici, UDK: 624.073.11, 2005.  
 [5] Cetkovic, M., *Primena Metode Konacnih Elemenata na Opstu Teoriju Laminatnih Ploca*, Magistarska teza, Građevinski Fakultet u Beogradu, 2005.